


# Identification of *MhLHC* gene family under iron (Fe) deficiency stress and functional characterization of *MhLHCB15* gene in *Malus halliana*

Yongjuan Dong, Zhongxing Zhang, Jiao Cheng, Xiaoya Wang, Wenbin Zhao, Donghai Zhang and Yanxiu Wang\* 

College of Horticulture, Gansu Agricultural University, Lanzhou 730070, China

\* Corresponding author, E-mail: [wangxy@gsau.edu.cn](mailto:wangxy@gsau.edu.cn)

## Abstract

Iron (Fe) plays a crucial role as a micronutrient in facilitating plant growth and development. Alterations in the availability of iron can trigger a response resulting in iron deficiency, ultimately affecting both plant growth and crop yield. A total of 33 light-harvesting chlorophyll a/b-binding protein (LHC) family members were identified based on the apple genome database. The physicochemical properties, gene structures, conserved motif compositions, evolutionary relationships, and chromosomal distributions were comprehensively analyzed. Subsequently, 15 genes were selected for quantitative reverse transcription PCR (qRT-PCR), and the results demonstrated that *MhLHCB15* significantly responded to Fe deficiency stress. Meanwhile, overexpression of *MhLHCB15* enhanced Fe deficiency tolerance in *A. thaliana* and apple calli, which evoked a variety of biochemical changes: transgenic *A. thaliana* displayed higher photosynthetic pigments content, photosynthetic efficiency, fluorescence parameters, and chlorophyll synthases expression compared to the wild-type (WT). Transgenic *A. thaliana* and apple calli had markedly greater levels of osmotic regulatory substances, enzyme activities, FCR activity, and expression of Fe uptake-related genes compared to the WT; however, the MDA content and reactive oxygen species (ROS) accumulation were less than the WT. Moreover, in this study, *MhLHCB15* interaction proteins SGR1, THF1, NDUFS1, CSN5b, and LHCA3 were screened, which provides a robust theoretical basis for analyzing the construction of the regulatory network of *MhLHCB15* under Fe deficiency stress.

**Citation:** Dong Y, Zhang Z, Cheng J, Wang X, Zhao W, et al. 2025. Identification of *MhLHC* gene family under iron (Fe) deficiency stress and functional characterization of *MhLHCB15* gene in *Malus halliana*. *Fruit Research* 5: e006 <https://doi.org/10.48130/frures-0024-0039>

## Introduction

Iron (Fe), a crucial mineral element necessary for the growth and development of plants is engaged in several biological processes such as photosynthesis, respiration, redox reactions, and nitrogen fixation<sup>[1,2]</sup>. Fe deficiency can limit chlorophyll synthesis, reduce photosynthetic rate, produce leaf chlorosis, and ultimately reduce fruit output and quality<sup>[3–5]</sup>. Although most soils contain sufficient total iron, the total iron available to plants may be insufficient depending on various soil factors. Fe deficiency can be caused by high pH and CaCO<sub>3</sub> concentration, ionic imbalance, and poor physical qualities such as high or low soil temperature, excessive humidity, poor soil aeration, and compaction, particularly in calcareous soils<sup>[6]</sup>. And approximately 40% of the world's soils are considered Fe limiting for plant growth<sup>[7]</sup>. The northwest Loess Plateau region of China is the best eco-climatic zone for apple cultivation<sup>[8]</sup>, the majority of orchards are calcareous soils with serious soil salinization, which has resulted in lower solubility of iron and nutrient deficiency<sup>[9]</sup>. Hence, Fe depletion severely constrained apple production in the region. To derive adequate iron for survival, plants have evolved a range of mechanisms to improve their ability to obtain iron from the soil<sup>[10,11]</sup>. The plants tightly control Fe uptake, translocation, and storage to maintain Fe homeostasis at the whole-plant level<sup>[1,12]</sup>. Most of these studies reported physiological and molecular components involved in iron acquisition and transport, such as *MxCS3* by Han et al.<sup>[13]</sup>, *MxNAS3* by Han et al.<sup>[14]</sup>, and *MxWRKY53* by Han et al.<sup>[15]</sup>

Photosynthesis is the basis of life on Earth, there are many heme- and Fe-S cluster-containing proteins working in the photosynthetic electron transport chain so iron (Fe) deficiency tends to cause severe photodamage<sup>[16]</sup>. The primary site of photodamage is in photosystem II (PSII)<sup>[17]</sup>, and hence plants modulate their absorption of light

energy by altering the size of the PSII-LHCII light-trapping antennae. The light-harvesting chlorophyll a/b-binding protein (LHC) family proteins encoded by nuclear genes act as antennae proteins and are crucial in light energy trapping and energy transfer as well as in response to adversity stresses<sup>[18,19]</sup>. The LHC gene family mainly contains two evolutionary taxa, LHCI and LHCII, which are associated with photosystem I (PSI) and PSII in the photosynthetic system, respectively<sup>[20]</sup>. The capture and transfer of photosynthetic energy in higher plants is primarily accomplished by the LHCI and LHCII<sup>[21,22]</sup>. LHCII, the predominant antenna protein found in plant PSII, efficiently converts the absorbed light energy into useable form, contributing significantly to plant photosynthesis. It facilitates the transfer and conversion of light energy, ensures the proper distribution of vesicle accumulation and excitation between the two photosystems, thereby offering photoprotection and aiding in the adaptation to diverse environmental conditions<sup>[23]</sup>. The most abundant LHCII, also referred to as the major LHCII, consists of LHCB1, LHCB2, and LHCB3 proteins<sup>[24]</sup>. The three minor LHCII proteins are LHCB4 (CP29), LHCB5 (CP26), and LHCB6 (CP24)<sup>[25,26]</sup>.

LHCB1 and LHCB2 can modulate the energy homeostasis distribution between PSI and PSII<sup>[27–29]</sup>. Andersson et al.<sup>[30]</sup> discovered that LHCB1 and LHCB2 proteins affect photosynthesis, which leads to a decline in light uptake by leaves, and a decrease in chlorophyll content in plants lacking the LHCB1 and LHCB2 genes, whereas plants with a light green coloration. Additionally, numerous *LHCII* genes have been found to regulate responses to abiotic stress<sup>[29,31]</sup>. Overexpression of *LeLHCB2* in tomato lessens the accumulation of ROS under low-temperature stress and enhances the low-temperature tolerance of transgenic tobacco<sup>[32]</sup>. The PSII antenna proteins CP29 and CP47 of *Salicornia europaea*, as well as several LHCII proteins, showed increased abundance in response to salt treatment, which enhanced the excitation energy capture capacity and

efficiency of PSII<sup>[33]</sup>. The expression of the *LHCB1* gene in *Oenanth javanica* was up-regulated under cold and drought stresses, which remarkably elevated photosynthesis<sup>[31]</sup>. The LHCI protein of *A. thaliana* also interacts with the Thylakoid Formation 1 (THF1) protein, in which silencing the THF1 gene can mitigate the degradation of the LHCI protein and delay the yellowing of plant leaves<sup>[34]</sup>. In previous studies, SGR1 was shown to specifically interact with LHCI to minimize the risk of photo-dynamism of these light-excitables intermediates by metabolically channeling chlorophyll breakdown pigments, thereby preventing accelerated plant death during leaf senescence<sup>[35]</sup>. In higher plants, chloroplast NDH (NADH dehydrogenase-like complex) interacts with two minor LHC I proteins, LHCA5 and LHCA6, contributing to the formation of the NDH-PS I super complex, which can mitigate the extent of plant damage under intense light conditions<sup>[36]</sup>. Ganeteg et al. found that LHCA5 interacts with other LHC I proteins (LHCA2, LHCA3)<sup>[37]</sup>, which suggests that genes from the same family members may have protein interactions and work together to regulate plant responses to adversity stress. Consequently, LHCI proteins perform an extremely important role in plant photosynthesis.

*Malus halliana* is a genus of apple native to the arid saline habitats of the Hexi Corridor in Gansu Province and has been found to have a certain Fe deficiency tolerance in long-term research<sup>[12,38]</sup>. The 33 *MhLHC* family members were screened to analyze them bioinformatically. The qRT-PCR assay indicated that *MhLHCB15* markedly responded to Fe deficiency stress. In this experiment, the *MhLHCB15* gene was cloned from *M. halliana*, as well as *MhLHCB15* transgenic apple calli and *A. thaliana* obtained by gene transformation and they were subjected to Fe-deficiency stress test and the physiological parameters were determined. Furthermore, the yeast two-hybrid (Y2H) technology was used to identify the proteins that interact with *MhLHCB15*, which provided a powerful rationale and reference for the analysis of the biological function of *MhLHCB15* under adversity stress and the construction of the regulatory network.

## Material and methods

### Plant material and treatment

The *M. halliana* plants were regularly transferred every 30 d onto a nutrient-rich solid medium called Murashige and Skoog (MS) at a temperature of 25 °C. This medium consisted of 0.5 mg/L of 6-BA and 0.1 mg/L of NAA. The solid medium, referred to as MS, comprised 4.43 g/L of MS powder obtained from Coolaber, Beijing, China. Additionally, it contained 30 g/L of sucrose and 7 g/L of agar, with the pH range of 5.8 to 6.0.

For gene expression analysis, seedlings of *M. halliana* were subcultured for about 20 d in rooting culture medium, composed of 1/2 MS powder, 0.4 mg/L NAA, and 7 g/L agar, pH 5.8–6.0. Once seedlings had developed roots, plants were selected and pre-cultured on MS medium for 7 d. After 7 d of culture, *M. halliana* were subjected to different abiotic stress treatments, which were Fe deficiency (0 μM Fe)<sup>[39]</sup>, drought stress (15% PEG 6000), low temperature (4 °C), and saline-alkali stress (200 mmol/L NaCl + NaHCO<sub>3</sub>). Three replicates of each treatment were conducted, with five plants per replicate. Leaves were carefully gathered at various time intervals: 0, 12, 24, 48, and 72 h, and placed in liquid nitrogen in a refrigerator at –80 °C for later use.

The yeast strain (Y2H Gold) and yeast medium were purchased from Coolaber Bio, Inc. The vectors pGBKT7 and pGADT7 were kindly donated by Prof. Wang Xiaofei from Shandong Agricultural University (Shandong, China).

### Identification of LHC genes in *M. halliana*

All the LHC family members were screened from the apple genome database. Subsequently, the transcript IDs were converted to corresponding gene IDs, and the corresponding genes were found in the Apple genome database. After obtaining the candidate genes, LHC members were further screened and validated using the Pfam and SMART databases, ultimately 33 LHC members were identified for subsequent analysis.

### Phylogenetic analysis and gene sequence analysis

To explore the evolutionary relationship between members of the apple LHC proteins, the phylogenetic tree was constructed based on amino acid sequences of the LHC family from both *A. thaliana* and *M. halliana*. *A. thaliana* LHC proteins were retrieved from the TAIR database. The MEGAX software was used to systematically analyze the LHC proteins of *A. thaliana* and *M. halliana*. Neighbor-Joining (NJ) was employed to predict the phylogenetic tree, which was subjected to a Bootstrap method with 1,000 replications. In addition, the physical and chemical properties and hydrophobicity predicted proteins were analyzed using ExPASy online tools (<https://web.expasy.org/protparam/> and <https://web.expasy.org/protscale/>). We utilized the online tool Plant-mPloc ([www.csbio.sjtu.edu.cn/bioinf/Cell-PLoc-2](http://www.csbio.sjtu.edu.cn/bioinf/Cell-PLoc-2)) to predict and analyze the subcellular localization. Additionally, we employed the MEME Suite online tool to analyze the conserved protein motifs (<https://meme-suite.org/tools/meme>). *Cis*-acting promoter elements were predicted and analyzed with the PLACE database ([www.dna.affrc.go.jp/PLACE](http://www.dna.affrc.go.jp/PLACE)). Finally, to determine chromosome distribution of the apple *MhLHC* gene family, annotation information on the Apple genome database was downloaded from the Phytozome database and gene distribution was visualized with TBtools.

### Quantitative real-time PCR

An RNA extraction kit (Accurate Biotechnology (Hunan) Co., Ltd.) was utilized to extract total RNA from the samples. Reverse transcription was performed using the *Evo M-MLV* RT Mix kit with gDNA Clean for qPCR (Accurate Biotechnology (Hunan) Co., Ltd.). About 1 μg of total RNA was transcribed into cDNA. Primers were designed by Shanghai Sangon Biological Engineering (China) based on sequences retrieved from the Apple genome database. Real-time PCR primer pairs are listed in [Supplementary Table S1](#). RT-PCR was performed using the cDNA of *M. halliana* as a template. The 2<sup>-ΔΔCT</sup> method was utilized for quantitative analysis of the data, with *MhGAPDH* and *AtActin* serving as the reference genes for qRT-PCR<sup>[40]</sup>. The reaction system contained: 10 μL 2 × SYBR Green Pro Taq HS (10 μmol/L), 1 μL upstream primers (10 μmol/L), 1 μL downstream primers, 2 μL cDNA template, and 6 μL RNase free water. The experimental setup included the following reaction parameters: pre-denaturation at 95 °C for 30 s, denaturation at 95 °C for 5 s, annealing at 60 °C for 30 s, and extension at 37 °C for 5 s, repeated for 50 cycles. Three replicates were performed for each sample.

### Gene cloning and vector construction

LHC family members induced by Fe deficiency were identified in the Apple genome database and compared to sequences at NCBI ([www.ncbi.nlm.nih.gov](http://www.ncbi.nlm.nih.gov)) to obtain the apple *MhLHCB15* (103429652). And then they were designed using DNAMAN. Forward primer: ATGGCAGCTTCCATGGCT and reverse primer: TCACTTCCGGGAA CAAAG. The PCR product was subjected to electrophoresis on 1% agarose gel to separate the fragments. The targeted gene fragment was then recovered from the gel and ligated with the pMD19-T cloned vector for sequencing. This was then transformed into *E. coli*, which was sequenced and sieved. The correct sequence of the *MhLHCB15* plasmid was extracted, digested with the restriction

enzymes *Sma* I and *Kpn* I, and connected to the pRI101 expression vector. Next, *E. coli* underwent transformation, and a positive colony was identified, which was further transformed into *Agrobacterium GV3101* using the freeze-thaw method for genetic transformation.

The specific primers SGR1, THF1, NDUFS1, CSN5b and LHCA3 were designed (Supplementary Table S1), according to the sequence (103444765, 103411255, 103426210, 103456101, 103444815) retrieved in the NCBI database. The cDNA of *M. halliana* was utilized as the template for RT-PCR amplification, and the amplified product was purified and sequenced. The pGADT7 vector was double digested with *EcoR* I and *BamH* I, and the correctly sequenced PCR purified and recovered products were ligated with the digested products and transformed into *E. coli* and a single clone was picked for colony PCR detection, and the positive clones were sequenced, and the pGADT7-SGR1/THF1/NDUFS1/CSN5b/LHCA3 recombinant plasmid was extracted after the correct sequencing.

### Agrobacterium-mediated transformation of *A. thaliana* and apple calli

*A. thaliana* seeds were obtained through genetic transformation following the method described by Hu et al.<sup>[41]</sup>. The seeds were treated with 75% ethanol for 5 min, followed by a 10 min treatment with 2.6% sodium hypochlorite. Subsequently, the seeds were rinsed with deionized water three to five times. The resistant plants were screened on MS medium containing 30 mg/L kanamycin and heterozygous transgenic plants were obtained. After three successive generations of screening, the homozygous transgenic plants of the T<sub>3</sub> generation were obtained.

Infection of apple calli was based on the method of Hu et al.<sup>[41]</sup>. After 15 d, calli of the same culture state were immersed in an infection solution with an OD value of 0.4 to 0.6 cultured in the dark (220 r/min) for 15–20 min, then filtered. The calli were placed on solid MS medium for 2 d and spread evenly on 250 mg/L Cef and 30 mg/L Kan resistance medium. They were screened for about 30 d on the plate until the transgenic calli was obtained. Then they were evenly distributed on 250 mg/L Cef and 30 mg/L Kan resistant medium for 3–5 times to obtain stable growth resistant calli. DNA was extracted and used for PCR identification.

### Treatment with Fe deficiency in *A. thaliana* and apple calli and physiological index measurement

The seeds of the wild-type (WT) and T<sub>3</sub> generation homozygous transgenic lines of *A. thaliana* were disinfected, vernalized at 4 °C for 3 d, grown on Fe sufficient (CK: 40 μM Fe) MS subculture medium for 10 d, then transferred to Fe deficient (–Fe: 0 μM Fe) MS medium for 20 d. Seedlings were placed in a light incubator (light 16 h/dark 8 h, 22 °C). Fe was provided in the form of Fe-EDTA. The wild-type and transgenic apple calli were placed on MS (CK: 40 μM Fe) succession medium containing 1.5 mg/L 2,4-D, 0.4 mg/L 6-BA for 10 d, and then transferred to Fe-deficient (–Fe: 0 μM Fe) MS medium for 20 d.

The photosynthetic parameters (Pn, Gs, Tr, and Ci) were measured on leaves using a portable photosynthesizer (LI-6400, LI-COR, Lincoln, NE, USA), with each treatment being replicated three times. The fluorescence parameters were assayed by the IMAG-ING-PAM chlorophyll fluorescence imager which was measured at the same time as the photosynthetic parameters, then through 30 min dark treatment, and the fluorescence parameters F<sub>0</sub>, F<sub>m</sub>, F<sub>v</sub>/F<sub>m</sub>, and q<sub>p</sub> were analyzed by Imaging Win Geg E soft-ware software.

The photosynthetic pigments content, including chlorophyll a (Chl a), chlorophyll b (Chl b), chlorophyll a+b (Chl a+b), and carotenoids (Car), was determined following the method described by Fitter et al.<sup>[42]</sup>. The soluble protein (SP) content was assayed by Caumas Brilliant Blue staining<sup>[43]</sup>. The content of soluble sugar (SS) in the leaves was determined using the Anthrone method<sup>[44]</sup>. The

activities of superoxide dismutase (SOD), peroxidase (POD) and catalase (CAT), H<sub>2</sub>O<sub>2</sub> content and O<sub>2</sub><sup>•-</sup> content was determined using a spectrophotometry kit from Suzhou Keming Biological (China).

The NBT and DAB staining were performed using the method of Romero-Puertas et al.<sup>[45]</sup>. Finally, following the method of Schikora & Schmidt<sup>[46]</sup>, the content of ferric chelate reductase (FCR) was calculated from absorbance measurements at 520 nm. The total Fe content was measured using the method of Mandal et al.<sup>[47]</sup>. Acidification analysis was based on the method of Zhao et al.<sup>[48]</sup>. Three biological replicates were performed for each treatment.

The expression of iron uptake-related genes (*AHA2*, *AHA8*, *FRO2*, *IRT1*, *FIT*, and *FER*) and chlorophyll synthases (*HEMA1*, *GSA1*, and *CAO*) was assayed using qRT-PCR, and the gene primers are shown in Supplementary Table S1.

### Extraction of DNA from transgenic *A. thaliana* and calli

The DNA of transgenic *A. thaliana* and apple calli were extracted using the SteadyPure Plant Genomic DNA Extration kit (Accurate Biotechnology (Hunan) Co., Ltd.).

### Construction of pGBKT7-*MhLHCB15* bait vector

The no-load line of the yeast BD vector used is pGBKT7 and the no-load line of the AD vector is of pGADT7 in this experiment. The specific primers *MhLHCB15*-BD (Supplementary Table S1) were designed. The cDNA of *M. halliana* served as the template for amplification using RT-PCR, and the resultant product underwent purification and sequencing. The pGBKT7 vector was double digested with *EcoR* I and *Sal* I, and the correctly sequenced PCR purified and recovered products were ligated with the digested products to transform into *E. coli*. Subsequently, a single clone was picked for colony PCR detection, after conducting sequencing on the positive clones, we proceeded to extract the recombinant plasmid pGBKT7-*MhLHCB15* once the sequencing results were confirmed as accurate.

### Decoy carrier self-activation assay

The pGBKT7-*MhLHCB15* and empty pGADT7 were transferred into yeast Y2H Gold, coated on SD/-Trp/-Leu solid medium, incubated inverted at 30 °C for 2 d, and then streaked on SD/-Leu/-Trp/-His/-Ade solid medium, incubated at 30 °C for 3–5 d to observe the growth of yeast colonies.

### Mating two-hybrid library screening

The specific steps were carried out with reference to the SOP instructions for yeast two-hybrid screening from Shanghai OE Biotech Co., Ltd.

### Positive clonal strain of yeast for PCR identification and sequencing

The above blue monoclonal yeast strain was subjected to bacteriophage PCR, and positive clones with bands were screened by agarose gel electrophoresis and subsequently sequenced. After completion of sequencing, BLAST tool in NCBI was used for comparative analysis to select the genes related to the function of *MhLHCB15* gene for one-to-one co-transfection verification.

### Validation of *MhLHCB15* and interacting proteins

The pGADT7-SGR1, pGADT7-THF1, pGADT7-NDUFS1, pGADT7-CSN5b, and pGADT7-LHCA3 vectors were simultaneously introduced into yeast Y2H Gold cells along with pGBKT7-*MhLHCB15*, individually, and set up negative controls (pGADT7 + pGKBT7, pGADT7 + pGKBT7-*MhLHCB15*, pGKBT7 + pGADT7-SGR1/THF1/NDUFS1/CSN5b/LHCA3) coated on SD/-Trp/-Leu plate growth. The transformation solution was diluted 10, 100, and 1,000 times and then spotted on SD/-Trp/-Leu/-His/-Ade/*X-α*-Gal plates and incubated for 3–5 d. The growth of yeast colonies and the color development were

observed to verify the interactions between *MhLHCB15* and the interacting proteins SGR1, THF1, NDUFS1, CSN5b, and LHCA3.

### Statistical analyses

The data were counted and processed using Excel 2019 and the data were analyzed using SE. Inter-group comparisons were made using the LSD method of one-way ANOVA ( $p < 0.05$ ). Statistical analyses were carried out using SPSS version 22.0 and figures were created using Origin 8.0 software.

## Results

### Identification of the *MhLHC* family members in apple and analysis of the physicochemical properties

A total of 33 typical *MhLHC* genes were derived using the apple genome database. They were named *MhLHCA1* to *MhLHCA10*, and *MhLHCB1* to *MhLHCB22* based on their chromosomal locations and known LHC genes in *Arabidopsis*. As shown in Supplementary Table S2, the number of encoded amino acids was relatively equal with an average of 265.12. Isoelectric points (pIs) of the proteins were in the scope of 4.54 to 9.46, aliphatic indices ranged from 74.14 to 99.57, and molecular masses (MW) covered the range of 6,272.21 to 38,200.48 Da. The positive residues are between 5 to 33, and the negative residues span from 5 to 34. Subcellular structural localization predictions revealed that all 33 LHC family proteins were located in chloroplasts.

### Phylogenetic analysis, structure, and conserved motif of apple LHC members

The phylogenetic analysis of 33 *MhLHC* protein sequences illustrated that the gene family can be categorized into three groups: Group I, Group II, and Group III (Fig. 1a). The results of the conserved motif analysis indicated all of Group I contained motif 1 to motif 10, and both Group II and Group III contained motif 1, motif 2, motif 4, motif 6, and motif 7 (Fig. 1b). There are at least two introns for *MhLHCB1*, *MhLHCB6*, *MhLHCB2*, *MhLHCB9*, *MhLHCA1*, *MhLHCA2*, *MhLHCA3*, *MhLHCA6*, and *MhLHCA9*, while *MhLHCB8*, *MhLHCB7*, *MhLHCB16*, *MhLHCB15*, *MhLHCB21*, *MhLHCB13*, *MhLHCB20*, and *MhLHCB10* contain only one exon (Fig. 1c).

### Chromosome distribution and collinearity analysis of the apple *MhLHC* genes

The chromosome location indicated that the apple *MhLHC* genes were asymmetrically distributed on 18 chromosomes (Supplementary Fig. S1a). There were five *MhLHC* genes located on the Chr17, with the maximum number, which was followed by three *MhLHC* genes, including in Chr05, Chr07, and Chr09, and lastly two *MhLHC* genes on Chr06, Chr08, Chr10, and Chr15. There were 10 covariant gene pairs between *MhLHC* genes (Supplementary Fig. S1b), which deserves special attention is the covariance of the *MhLHCB4* and *MhLHCB17* genes. Simultaneously, *MhLHCA10*, *MhLHCB20*, *MhLHCB23*, *MhLHCB22* have co-linear relationship with *MhLHCB7*, *MhLHCB8* and *MhLHCA5*, *MhLHCB14*, respectively. In addition, *MhLHCB3* and *MhLHCB10* with *MhLHCB11*, *MhLHCA9* and *MhLHCA6*, *MhLHCB21* and *MhLHCB13* have covariate relationships. Moreover, there was a covariance between *MhLHCA7* and *MhLHCA2*, *MhLHCB19* and *MhLHCB12*, *MhLHCA8* and *MhLHCA4*, and *MhLHCB18* with *MhLHCB5*, for each of them. The findings presented in this study reveal that the production of *MhLHC* genes could potentially arise from gene duplication occurrences, where segmental duplication events acted as an impelling role in the evolution of LHC proteins.

### Phylogenetic analysis of LHC family members

Aiming to explore the putative function of the predicted *M. halliana* LHC, we allocated them to *A. thaliana* LHC proteins with known functions. A total of 33 *MhLHC* proteins in *M. halliana* and 19 *AtLHC* proteins in *A. thaliana* were analyzed. The phylogenetic distribution indicated that the LHC proteins can be classified into three clades (named Group I, Group II, and Group III) according to their sequence similarity. Among them, Group III is more distributed, which contains 31 members, Group II includes 14 members, and Group I consists of the least number of members, with seven members (Supplementary Fig. S2).

### Analysis of *cis*-acting elements in the promoter region of the *MhLHC* gene

To comprehend the *cis*-acting elements contained in the promoter region of the apple *MhLHC* genes, 2-kbp sequences upstream of the *MhLHC* genes were taken and analyzed. The results demonstrated that multiple promoter regions of the *cis*-acting element-rich

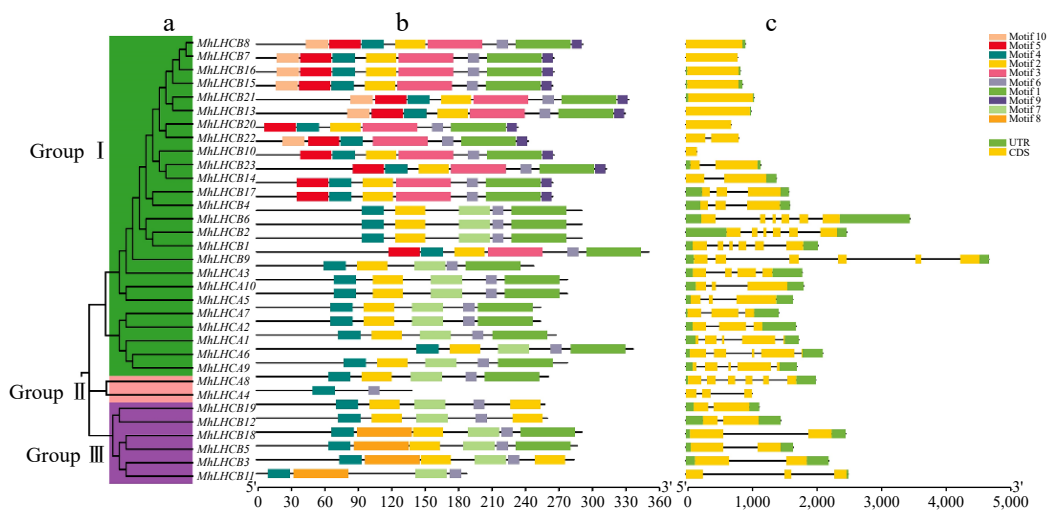


**Fig. 1** Phylogenetic relationships, architecture of conserved protein motifs, and gene structure in *MhLHC* gene family from apple. (a) The phylogenetic tree was constructed based on the full-length sequences of *MhLHC* family proteins using MEGA-X software. Details of clusters are shown in different colors. (b) The motif composition of *MhLHC* proteins. The motifs, numbers 1–10, are displayed in different colored boxes. The scale at the bottom can be used to estimate the length of the protein. (c) Exon-intron structure of *MhLHC* genes family. Green boxes represent untranslated 5'- and 3'-regions; yellow boxes denote exons; black lines indicate introns.

*MhLHC* genes were responsive to auxin, GA, ABA, SA, MeJA, drought, low temperature, and light (Supplementary Fig. S3), which suggested that the functions of the *MhLHC* may include a range of biological processes such as the regulation of plant growth and development, phytohormone signaling, and plant resistance to stresses.

**Expression of apple *MhLHC* genes family members under different abiotic stresses**

Fifteen *MhLHC* genes that are homologous to respond to abiotic stresses in *A. thaliana* were selected and analyzed their relative expression under abiotic stresses such as Fe deficiency, drought, low temperature, and saline-alkali, aiming to understand the expression patterns of apple *MhLHC* family genes under different abiotic stresses (Fig. 2). Among all *MhLHC* genes, *MhLHCB15*, *MhLHCA3*, *MhLHCA10*, and *MhLHCB11* expression were remarkably up-regulated, with a maximum of 72 h under Fe deficiency, drought, low temperature, and saline-alkali stress treatments compared to 0 h, of which *MhLHCB15* expression was markedly elevated. The expression of *MhLHCA1* and *MhLHCA7* genes were reduced under low-temperature stress, and saline-alkali stress, in which *MhLHCA7* expression was dramatically raised after 12 h of Fe deficiency and

drought stress treatments. It indicates that there are differences in the response mechanisms to abiotic stresses among the genes of the *MhLHC* family, although most of the genes have similar response mechanisms to different abiotic stresses. In summary, the expression changes of other genes under abiotic stress were less notable than those of *MhLHCB15* under Fe deficiency, implying that *MhLHCB15* might be involved in the response to Fe deficiency stress.

**Analysis of the *MhLHCB15* gene**

The cDNA of *M. halliana* seedlings was used as a template, and a 795 bp band was obtained (Supplementary Fig. S4), encodes a total of 264 amino acids and possesses an isoelectric point of 5.29, thereby classifying it as an acidic protein. In addition, the positive and negative residues of *MhLHCB15* are 21 and 26, respectively, and the average hydrophobicity is  $-0.020$ , which is a hydrophilic protein (Supplementary Table S1). This indicates that the protein encoded by *MhLHCB15* is an acidic hydrophilic protein. Sequence alignment was carried out to compare the amino acid sequences encoded by *MhLHCB15* with those of other organisms, which showed a certain degree of difference at the N-terminal and high similarity at the C-terminal (Supplementary Fig. S5). Phylogenetic analysis was performed on the amino acid sequences encoded by *MhLHCB15* and

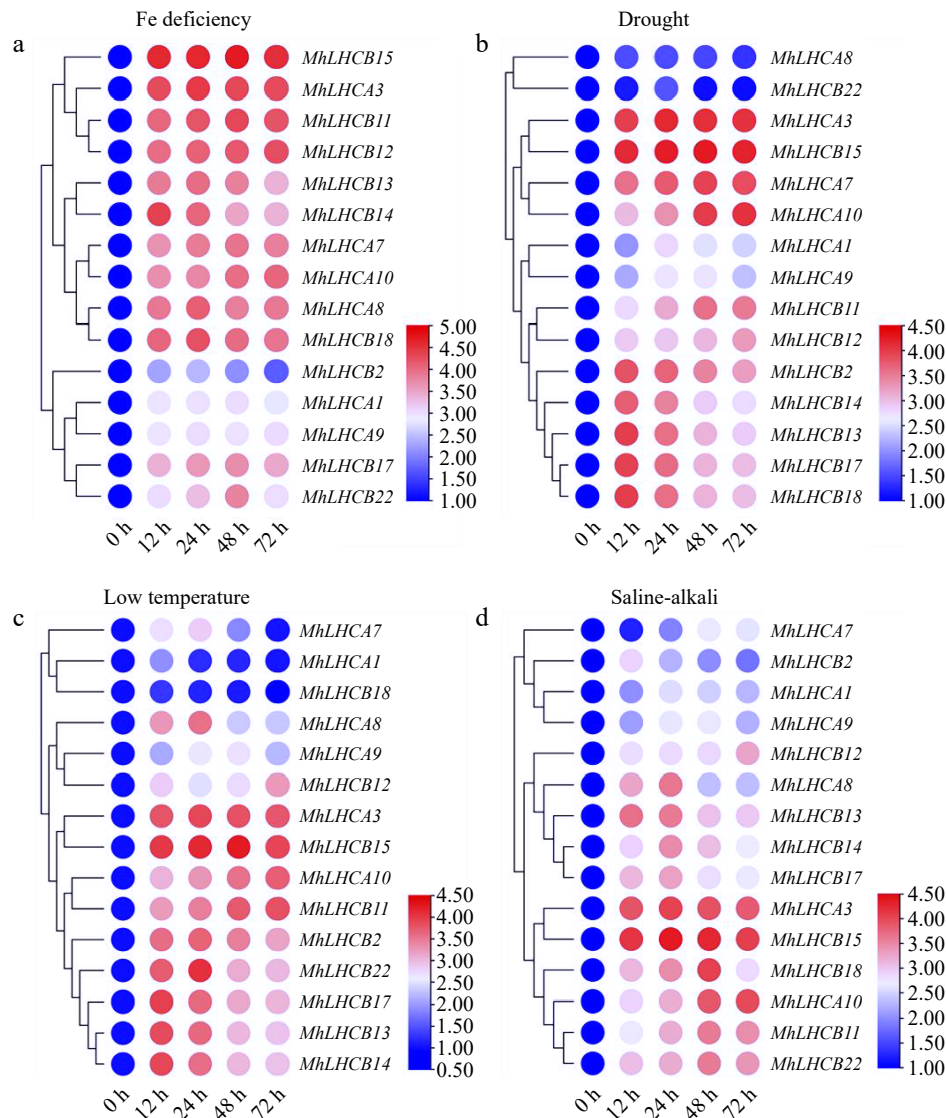


**Fig. 2** Heat map relative expression levels of *MhLHC* genes in *M. halliana* leaf cultures on abiotic stress medium at 0, 12, 24, 48, and 72 h. (a) Fe deficiency (0  $\mu$ M Fe), (b) drought stress (15% PEG 6000), (c) low temperature (4  $^{\circ}$ C), (d) saline-alkali stress (200 mmol/L NaCl + NaHCO<sub>3</sub>).

genes from similar species. *MhLHCB15* showed high homology to a protein from *Pyrus × bretschneideri* (97%) (Supplementary Fig. S6).

The *cis*-elements in the sequence 2,000 bp upstream of the *MhLHCB15* was analyzed and multiple *cis*-elements associated with abiotic stress were found (Table 1), which suggests that *MhLHCB15* may exert a crucial part in response to diverse stresses.

### Identification of overexpressing *A. thaliana* and apple calli

The DNA of transgenic *A. thaliana* and overexpressed apple calli were extracted and characterized by PCR. As shown in Fig. 3a, b, and the size of the detected electrophoretic bands is consistent with the size of the *MhLHCB15* fragment. The expression levels of *MhLHCB15* in transgenic *A. thaliana* and overexpressed apple calli were detected by qRT-PCR. In comparison to the plants with WT plants, the expression levels of *MhLHCB15* were higher in transgenic *A. thaliana* and overexpressed apple calli, indicating that *MhLHCB15* was overexpressing (OE) in both (Fig. 3c, d).

### Tolerance of *MhLHCB15* overexpressed *A. thaliana* to Fe deficiency

To determine whether *MhLHCB15* plays a role in response to Fe deficiency, three transgenic *A. thaliana* lines (OE-1, OE-2, OE-4) and the wild-type (WT) control were grown for 30 d under Fe-sufficient conditions, then shifted to Fe-sufficient or Fe-deficient conditions

for another 20 d. This is shown in Fig. 4, *A. thaliana* grew vigorously in normal conditions, and the growth rate was basically the same, while growth was inhibited to varying degrees when exposed to Fe-deficiency stress. Compared with transgenic *A. thaliana*, the WT control showed more obvious chlorosis and wilting.

As shown in Fig. 5a–d, the three transgenic lines exhibited a remarkable increase in Chl a, Chl b, Car, and Chl a+b under Fe-deficient conditions when compared with WT, whereas they did not differ from WT under Fe-sufficient conditions. As can be seen from Fig. 5e–h, Tr, Gs, and Pn of leaves showed a continuous decrease after Fe deficiency, though it was lower in transgenic plants compared to WT. However, the Ci content tended to be elevated, and the increase was more pronounced in the WT plants. The qP, F0, Fm, and Fv/Fm of both transgenic and WT plants exhibited a declining trend under Fe deficiency, with less of a decrease in the transgenic plants (Fig. 5i–l).

The SOD, POD, and CAT activities of transgenic and WT *A. thaliana* have been measured (Supplementary Fig. S7a–c). Under Fe-deficient conditions, these antioxidant enzyme activities (SOD, POD, and CAT) were much higher in transgenic *A. thaliana* than in WT controls. Meanwhile, the soluble sugar (SS) and soluble protein (SP) contents of the *MhLHCB15*-OE lines and wild-type *A. thaliana* were reduced in iron deficiency, whereas the contents of the transgenic lines were significantly higher than those of the WT (Supplementary

**Table 1.** *Cis*-elements in the genomic sequence 2,000 bp upstream of the *MhLHCB15*.

<i>Cis</i> -acting element	Sequence	Start sites (bp)	End sites (bp)	Function
G-box	TACGTG	+601	+607	<i>Cis</i> -acting regulatory element involved in light responsiveness
LTR	CCGAAA	+342	+348	<i>Cis</i> -acting element involved in low-temperature responsiveness
ABRE	ACGTG	+602	+607	<i>Cis</i> -acting element involved in the abscisic acid responsiveness
AuxRR-core	GGTCCAT	+1,451	+1,458	<i>Cis</i> -acting regulatory element involved in auxin responsiveness
P-box	CCTTTTG	+1,278	+1,285	Gibberellin-responsive element
ARE	AAACCA	−1,067	−1,073	<i>Cis</i> -acting regulatory element essential for the anaerobic induction
MBS	CAACTG	+1,334	+1,340	MYB binding site involved in drought-inducibility
TGACG-motif	TGACG	−655	−660	<i>Cis</i> -acting regulatory element involved in the MeJA-responsiveness

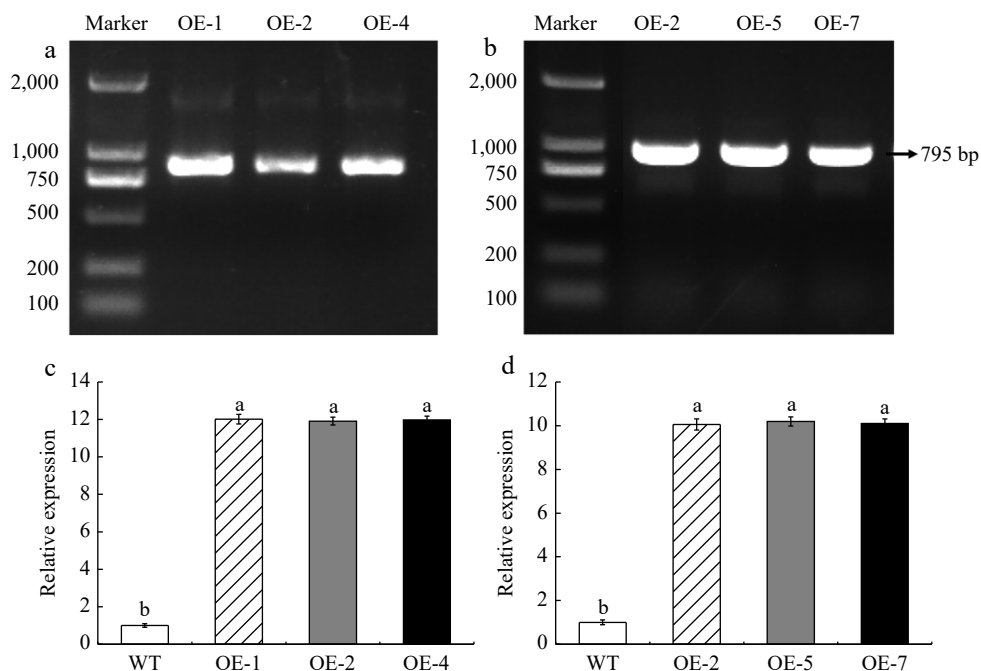


**Fig. 3** Identification of genetically modified material. (a) DNA identification of transgenic *A. thaliana*. (b) DNA identification of overexpressed apple calli. (c) Expression level of *MhLHCB15* in *A. thaliana*. (d) Expression level of *MhLHCB15* in apple calli. Resistance of transgenic *MhLHCB15* *A. thaliana* and apple calli to Fe (iron) deficiency stress. Different letters above the bars indicated significant differences ( $p < 0.05$ ) as assessed by one-way ANOVA and the least significant difference (LSD) test.

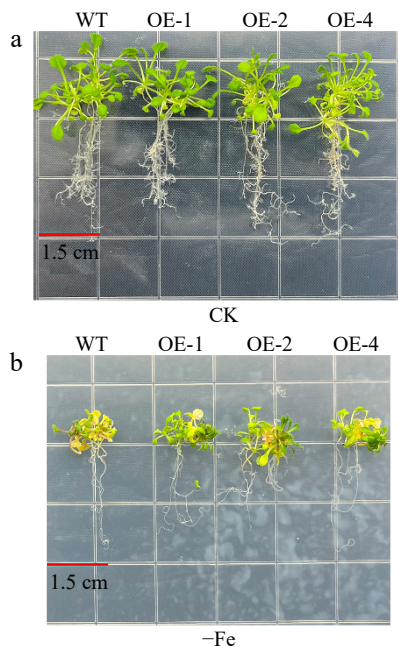


**Fig. 4** The phenotypes of *MhLHCB15* transgenic and wild-type (WT) *A. thaliana* grown for 20 d on Fe-sufficient or Fe-deficient medium. (a) Fe-sufficient (CK), (b) Fe-deficient (-Fe).

Fig. S7d–e). In addition, both Pro and MDA were remarkably elevated under Fe deficiency, and the Pro content was greater in the *MhLHCB15*-OE *A. thaliana* than in the WT strain, while the MDA content was also below that of the WT (Fig. 6f, g). The results demonstrated that the  $\text{Fe}^{2+}$  content and FCR activity were substantially higher than those of the WT control (Supplementary Fig. S7h–i). Eventually, the accumulation of  $\text{H}_2\text{O}_2$  and  $\text{O}_2^-$  in transgenic *A. thaliana* leaves in Fe-deficient conditions was significantly lower than that of the WT, with no obvious difference under normal conditions (Fig. 6a–d).

To further investigate the role of *MhLHCB15* in the Fe signaling pathway, the expression levels of Fe uptake-related genes and chlorophyll synthase in *A. thaliana* plants overexpressed *MhLHCB15* were examined by qRT-PCR (Supplementary Fig. S8). The results illustrated that the expression levels of Fe uptake-related genes (*AtAHA2*, *AtAHA8*, *AtFRO2*, *AtIRT1*, *AtFIT*, and *AtFER*) and chlorophyll synthesizing enzymes (*AtHEMA1*, *AtGSA1* and *AtCAO*) were decreased in overexpressed *A. thaliana* plants under Fe deficiency stress, but the expression of *MhLHCB15*-OE was higher than that of WT. All the above results indicated that *MhLHCB15* enhanced the tolerance of *A. thaliana* under Fe deficient stress.

### Tolerance of *MhLHCB15* overexpressed apple calli to Fe deficiency

It is clear from Fig. 7a, b that there was no apparent difference in the growth status of overexpressed and WT apple calli under Fe-sufficient conditions. Nevertheless, the growth status of overexpressed and WT apple calli varied greatly under Fe deficient conditions and the overexpressed calli performed better than the WT apple calli.

The POD, SOD, and CAT activities of transgenic lines (OE-2, OE-5, and OE-7) diverse from those of WT apple calli under Fe deficiency stress, whose enzyme activities were considerably higher than those of the WT (Supplementary Fig. S9a–c). It is obvious from Supplementary Fig. S9d, e that the content of osmoregulatory substances (SS and SP) in *MhLHCB15*-OE apple calli was remarkably decreased in iron deficiency, whereas the content in transgenic apple calli was notably superior to those of the WT. In parallel, the transgenic lines

Pro content was more than that of WT, while the MDA content was remarkably inferior to that of WT (Supplementary Fig. S9f–g). It is evident from Supplementary Fig. S9h–i that the accumulation of  $\text{H}_2\text{O}_2$  and  $\text{O}_2^-$  in overexpressed apple calli was markedly less than that of the WT at Fe deficiency, which was not appreciably dissimilar under normal conditions. Meanwhile, the transgenic lines with higher values of FCR activity and total Fe content when compared to the WT control lines (Supplementary Fig. S9j–k). In additionally, bromocresol violet staining in yellow indicated that the *MhLHCB15* transgenic calli pumped more  $\text{H}^+$  into the medium under Fe deficient conditions compared with the WT control (Fig. 8).

To further explore the role of *MhLHCB15* in the Fe signaling pathway, the expression levels of Fe uptake-related genes (*MhAHA2*, *MhAHA8*, *MhFRO2*, *MhIRT1*, *MhFIT*, and *MhFER*) were assayed in overexpressed apple calli *MhLHCB15* by qRT-PCR (Supplementary Fig. S10). In a word, these results demonstrate that homologous expression of *MhLHCB15* in apple calli can respond to Fe deficiency and reinforce its tolerance to stress.

### Construction of decoy vectors pGBKT7-*MhLHCB15* and self-activation assays

The results showed successful amplification of the target bands of approximately 795 bp (Supplementary Fig. S11a), which indicated the successful construction of the recombinant bait vector pGBKT7-*MhLHCB15*. The bait vector and positive control were then transferred into yeast Y2H gold receptor cells to verify the self-activation activities. It showed that the bacterial fluids containing the bait vector and the positive control could grow normally in SD/-Trp/-Leu medium, but only the positive control had blue colonies in SD/-Trp/-Leu/-His/-Ade/ $\alpha$ -Gal medium and the bait vector could not grow (Fig. 9a), which demonstrated that the bait vector did not have self-activation activity and it could be used for the screening of interacting proteins.

### pGBKT7-*MhLHCB15* decoy protein library screening and PCR assay

A total of 84 monoclonal strains were screened by Mating two-hybridization on SD/-Ade/-His/-Leu/-Trp plates using pGBKT7-*MhLHCB15* as the bait protein, and validated on SD/-Ade/-His/-Leu/-Trp/ $\alpha$ -gal plates, and found that a total of 56 strains could grow spots or turn blue, and PCR on PCR of these strains yielded 29 products (Fig. 9b), totaling 10 bands of inconsistent size. Sequencing revealed that a total of five corresponding genes were obtained. A comparison by NCBI revealed that most of the proteins were related to abiotic stress and photosynthesis, which contained SGR1 (STAY-GREEN), THF1 (Thylakoid Formation 1), NDUFS1 (NADH dehydrogenase [ubiquinone] iron-sulfur protein 1), CSN5b (COP9 signalosome complex subunit 5b), and LHCA3 (Light-harvesting chlorophyll a/b).

### Yeast point-to-point hybridization to verify *MhLHCB15* with interacting proteins

The SGR1, THF1, NDUFS1, CSN5b, and LHCA3 were amplified by PCR and sequenced after ligating the pGADT7 vector, and the sequencing results were consistent with the colony PCR results, with the band sizes of 852, 888, 2,250, 1,104, and 744 bp, respectively (Supplementary Fig. S11b–f), and the pGADT7 vector was successfully constructed. The pGBKT7 was co-transfected with the recombinant plasmid pGADT7-SGR1/THF1/NDUFS1/CSN5b/LHCA3 into Y2HGold yeast receptor cells. As can be seen in Fig. 9a, white yeast strains grew on SD/-Trp/-Leu plates but not on SD/-Trp/-Leu/-Ade/-His plates, which indicated that none of the SGR1, THF1, NDUFS1, CSN5b and LHCA3 genes were self-activating.

When the candidate interacting proteins SGR1, THF1, NDUFS1, CSN5b, and LHCA3 were co-transfected into yeast with pGBKT7-*MhLHCB15* bait vector, respectively, which displayed that all the

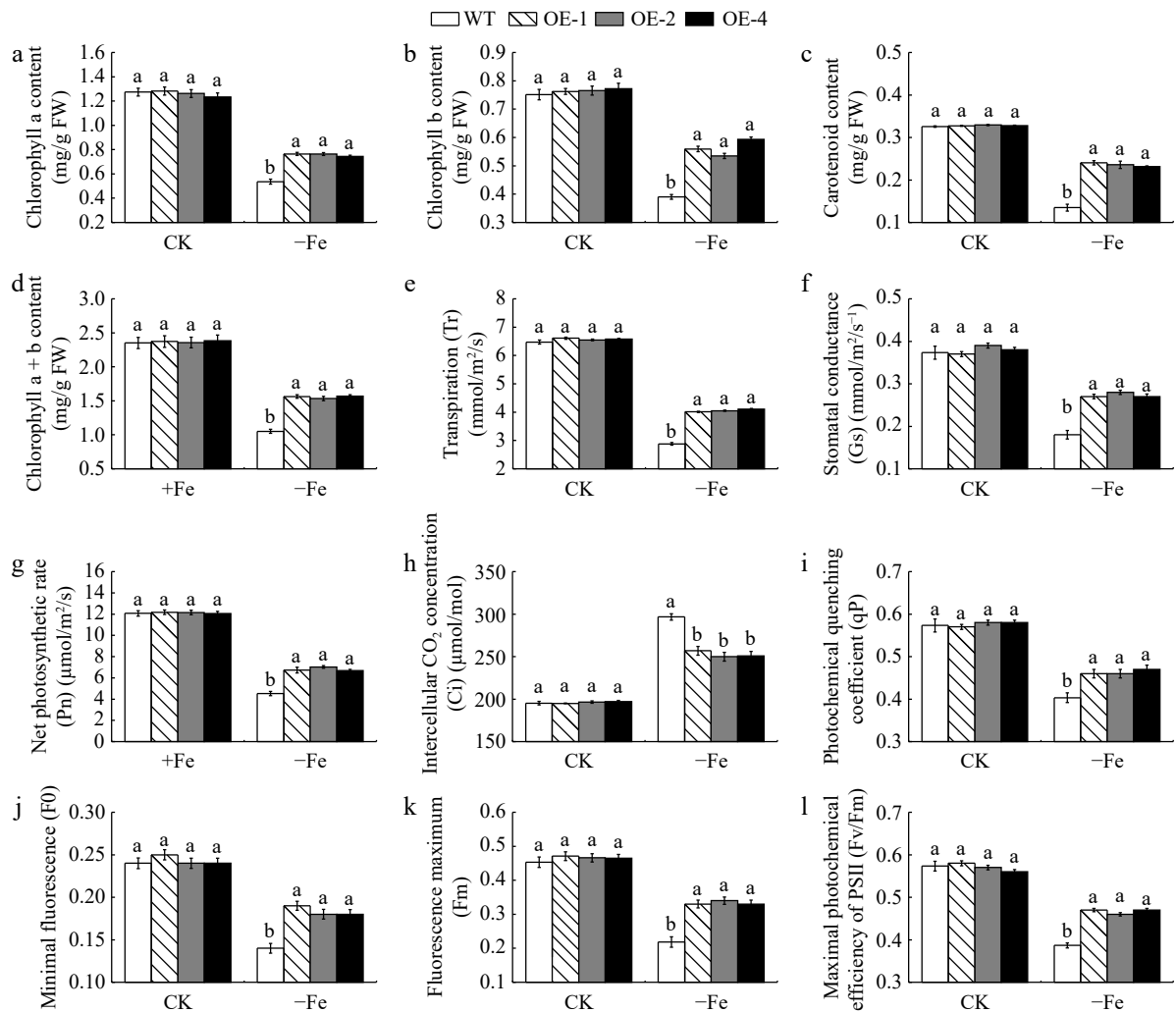


**Fig. 5** The photosynthetic pigment content and photosynthetic fluorescence parameters of *MhLHCB15* transgenic and wild type (WT) *A. thaliana* grown for 20 d under Fe-sufficient (CK) or Fe-deficient (-Fe) conditions. (a) Chlorophyll a content, (b) chlorophyll b content, (c) carotenoid content, (d) chlorophyll a+b content, (e) transpiration (Tr), (f) stomatal conductance (Gs), (g) net photosynthetic rate (Pn), (h) intercellular CO<sub>2</sub> concentration (Ci), (i) photochemical quenching coefficient (qP), (j) minimal fluorescence (F0), (k) fluorescence maximum (Fm), (l) maximal photochemical efficiency of PSII (Fv/Fm). Different lowercase letters showed significant difference at the level of  $p < 0.05$ .

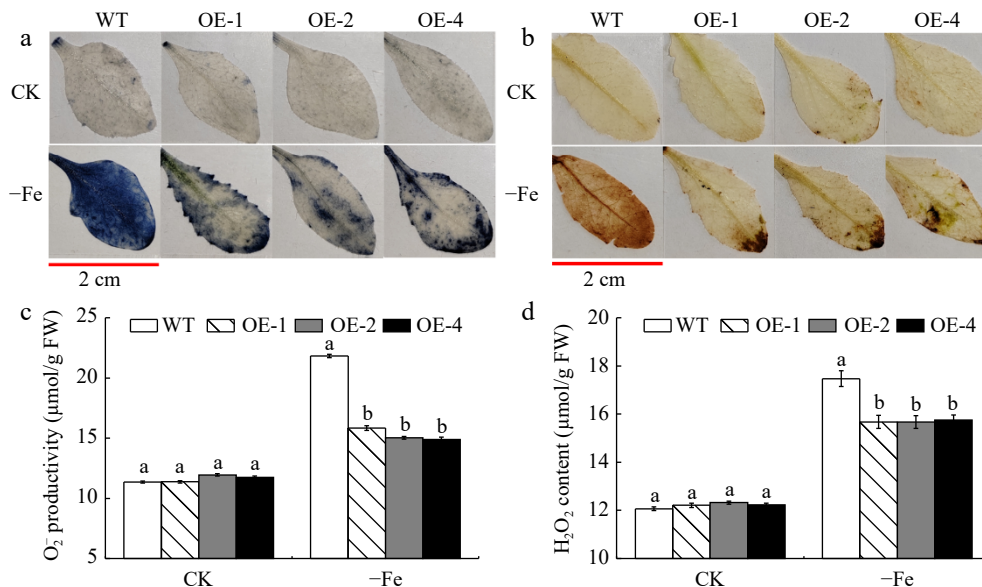


**Fig. 6** The accumulation of reactive oxygen species (ROS) of *MhLHCB15* transgenic and wild type (WT) *A. thaliana* grown for 20 d under Fe-sufficient (CK) or Fe-deficient (-Fe) conditions. (a) NBT staining, (b) DAB tissue staining, (c) O<sub>2</sub><sup>-</sup> content, (d) H<sub>2</sub>O<sub>2</sub> content.



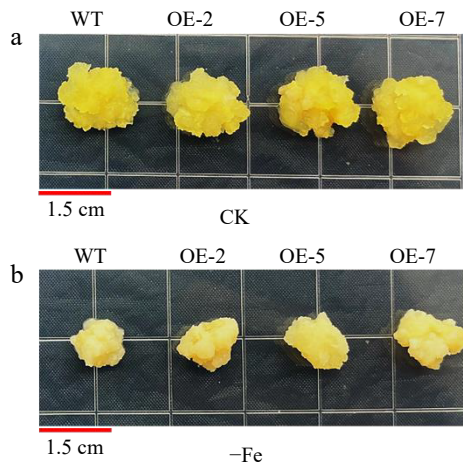


**Fig. 7** Phenotypes of overexpressed *MhLHCB15* and wild-type (WT) control apple calli grown on Fe-sufficient or Fe-deficient media for 20 d. (a) Fe-sufficient (CK), (b) Fe-deficient (-Fe).

colonies were able to grow on SD/-Trp/-Leu/-His/-Ade/X- $\alpha$ -Gal plates and turned blue (Fig. 9c), thus further confirming that the two proteins interacted with the *MhLHCB15* proteins in yeast.

## Discussion

### Identification of the LHC gene family in *M. halliana*

Light trapping is the utmost crucial part of the photosynthesis process, and it is mediated by LHC<sup>[49]</sup>, a plant-specific family of proteins that are mainly localized in the chloroplast-like vesicle membranes. They bind to the pigments to form the light-trapping pigment-protein complexes, which are involved in the collection and transport of light energy during photosynthesis<sup>[50]</sup>. The LHC gene family has been extensively studied in model plants such as *Arabidopsis* (*Arabidopsis thaliana* L.)<sup>[51]</sup> and rice (*Oryza sativa* L.)<sup>[52]</sup>. The LHC gene family is thought to be involved in the regulation of plant growth and development, the repair of light damage in the photosynthetic system, as well as in the response to various adversity stresses<sup>[18,19,53]</sup>. The levels of gene expression for the majority of *ZmLHCA* and *ZmLHCB* genes in *Zostera marina* are reduced when exposed to salt and low-temperature stress, consequently impacting the process of photosynthesis<sup>[54]</sup>. In *A. thaliana*, low concentrations of ABA promote the expression of *AtLHCB1-6*, while high concentrations inhibit the expression of *AtLHCB1-6* in response to the regulation of the external environment, especially adversity stress<sup>[55]</sup>, and down-regulation of the expression of *AtLHCB1-LHCB6* affects stomatal responses to ABA, thus leading to a decrease in the ability of plants to tolerate drought<sup>[29]</sup>. Nevertheless, the study of related LHCII proteins in resistance to stress and disease in *M. halliana* has not yet been reported.

In the present study, 33 members of the LHC gene family in apple were investigated based on the apple genome database and bioinformatics analysis. The 33 *MhLHC* genes exhibited some differences in their physical and chemical properties. In addition, many studies have shown that subcellular location is critical for the biological function of the identified sequences, especially functional sequences related to the regulation of gene expression<sup>[56]</sup>. The present study demonstrated that 33 *MhLHC* genes were predicted to be located in chloroplasts. Through phylogenetic tree analysis, 33 *MhLHC* genes were divided into three groups. To further determine the relationship between *MhLHC* genes in apple, the structure diagram of conserved elements was established by MEME software, 33 *MhLHC* genes have ten conservative motifs, which may lead to functional diversity<sup>[57]</sup>. Although the LHC proteins in apples vary in length, the clustered LHC proteins share the same protein motif location and gene structure. It is consistent with previous studies of the LHC family in the kiwifruit<sup>[58]</sup>, which indicated that this family was highly conserved during evolution. The LHC gene is more widely distributed on the Apple genome database and is most abundant on Chr17. At last, 10 pairs of genes were identified with segmental duplications. These outcomes revealed that the duplication events may contribute to the evolution of *MhLHC* genes.

### Overexpression of *MhLHCB15* enhanced tolerance to Fe deficiency in transgenic *A. thaliana* and apple calli

Iron is an essential trace element for plant growth. Any defect in Fe availability leads to a Fe deficiency reaction that causes leaf chlorosis and disrupts photosynthesis, affecting plant growth and crop yield<sup>[4]</sup>. The LHC is widely involved in the capture and transfer of light energy, leaf development, maintenance of vesicle membrane structure, and various stress responses<sup>[59,60]</sup>. For instance, overexpression of the *LHCB2* gene in tobacco enhanced tolerance to low temperatures<sup>[32]</sup>. Fe deficiency induces phosphorylation of *HvLHCB1* proteins, leading to their migration from grana stacks to stroma thylakoid membranes, thereby optimizing the excitation balance between PSII and PSI<sup>[61]</sup>. To summarize, LHC has a vital function that regulates gene expression in response to environmental stresses.

In this study, the expression patterns of 15 *MhLHC* genes in the leaves of *M. halliana* were examined by qRT-PCR validation, in which the expression of *MhLHCB15* changed dramatically under Fe deficiency stress. Transgenic *A. thaliana* with ectopically expressed *MhLHCB15* and homologous overexpressed apple calli were obtained. The photosynthetic pigments are critical for the absorption, transmission, and transformation of light<sup>[62]</sup>. It was found that the photosynthetic pigments content (Chl a, Chl b, Car, and Chl a+b) of transgenic *A. thaliana* under Fe deficiency stress was remarkably higher than that of WT, which indicated that the photosynthetic system of WT plants was more sensitive to Fe deficiency. It has been shown that the factors affecting the efficiency of plant photosynthe-

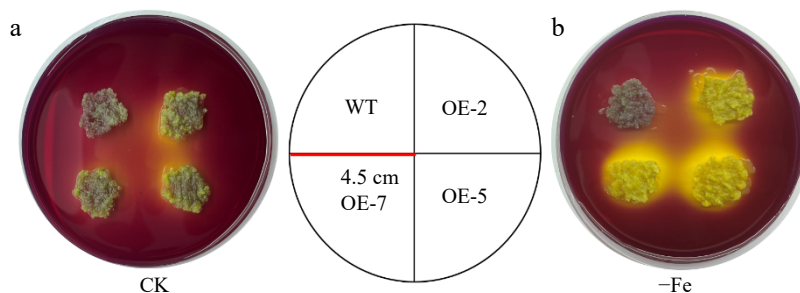


**Fig. 8** Acidification analysis of overexpressed *MhLHCB15* and wild-type (WT) control apple calli on medium containing the pH indicator dye bromocresol violet. A yellow color around apple calli indicates acidification. (a) Fe-sufficient (CK), (b) Fe-deficient (-Fe).

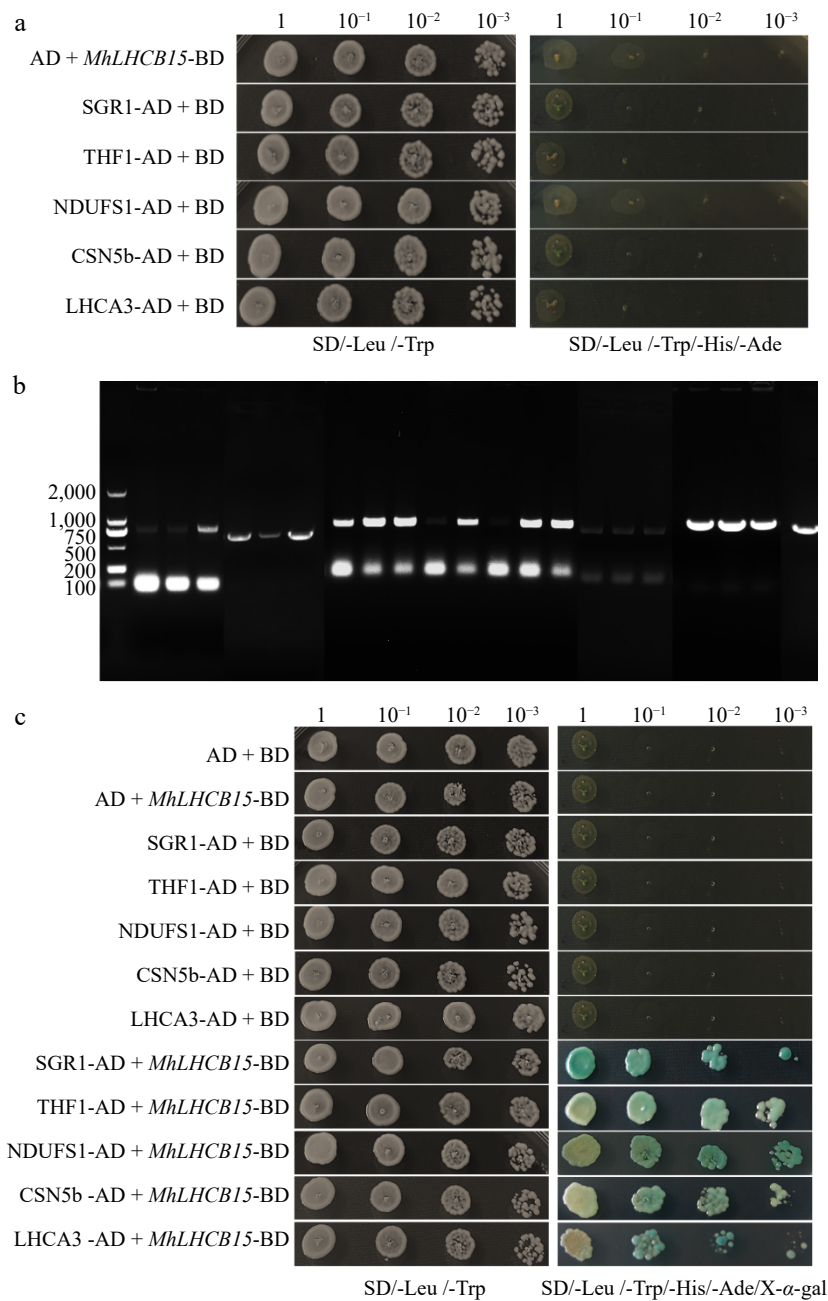


**Fig. 9** (a) The self-activations test of *MhLHCB15*, SGR1, THF1, NDUFS1, CSN5b, and LHCA3 proteins, (b) amplified fragments of selected genes for *MhLHCB15* library screening, (c) interaction verification between pGBKT7-*MhLHCB15* and interacting protein.

sis include stomatal limitation and non-stomatal limitation<sup>[63]</sup>. When Gs and Ci decreased at the same time, the decline in Pn was mainly caused by stomatal limiting factors, whereas if the decrease in Pn was accompanied by an increase in Ci, the main restricting factors for photosynthesis were non-stomatal factors<sup>[64]</sup>. In this work, Pn, Gs, and Tr decreased notably after Fe deficiency stress. On the contrary, Ci increased remarkably, which indicated that non-stomatal limitation under Fe deficiency stress was one of the main reasons for the decrease of Pn. The leaf chlorophyll fluorescence parameter can be used as an effective characterization to measure the strength of the plant's ability to respond to adversity stress<sup>[65,66]</sup>. This experiment showed that qP, F0, Fm, and Fv/Fm of transgenic *MhLHCB5*-OE leaves under Fe deficiency stress showed a continuous decreasing trend, illustrating that the PSII reaction centers of the plants received damage and the electron transfer rate of plant leaves slowed down under Fe deficiency stress, and the PSII damage in

*MhLHCB5*-OE was comparatively milder than in WT. These results are similar to those of Ali et al.<sup>[67]</sup> in winter wheat, indicating that *MhLHCB15* overexpression maintains photosynthetic electron transport in PSII, which in turn allows the plant to maintain a high photosynthetic efficiency with a high light-trapping capacity.

The SOD, CAT, and POD in plants facilitate the scavenging of ROS, thereby reducing the extent of membrane damage<sup>[68]</sup>. In the present study, it was revealed that the POD, SOD, and CAT activities of transgenic *A. thaliana* and apple calli were remarkably higher than those of WT under Fe deficient conditions, which meant that the *MhLHCB5*-OE had a stronger ability to scavenge reactive oxygen species (ROS) than WT, thus maintaining the stability of the membrane system. When plants are subjected to adversity, ROS are accumulated, thus disrupting cell membranes, and exocytosis of inclusions<sup>[69]</sup>. It was observed that H<sub>2</sub>O<sub>2</sub> and O<sub>2</sub><sup>-</sup> accumulation in transgenic *A. thaliana* leaves was markedly less than in WT under Fe

deficiency, and these findings align with the outcomes obtained from staining experiments using DAB and NBT, thus confirming that overexpression of *MhLHCB15* enhances ROS scavenging capacity.

Soluble sugars and soluble proteins are essential signaling substances that are evoked to accumulate in plants in response to adversity stresses<sup>[70]</sup>. The findings revealed that the overexpressing lines accumulated more SS and SP contents than WT under Fe deficiency conditions, which indicated that the *MhLHCB15*-OE accumulated more osmoregulatory substances to alleviate the damages caused by Fe deficiency stress to the plants. Pro, as a very critical osmotic regulator, acts to stabilize the plant cell structure<sup>[71]</sup>. The Pro content of *MhLHCB15*-OE exhibited an upslope after Fe deficiency stress, which demonstrated that Fe deficiency stress caused severe osmotic stress to plants and a large amount of Pro was accumulated in the plant cells to regulate the osmotic stress injury. The magnitude of damage to the membrane system was detected by the MDA content, which can be inferred from the plant's stress tolerance<sup>[72]</sup>. Following Fe deficiency stress, the MDA levels in the transgenic lines exhibited a decrease when compared to the WT plants, which demonstrated less cell membrane damage and enhanced resistance in *MhLHCB15*-OE.

The Fe<sup>2+</sup> content of leaves is a pivotal factor that influences the chlorophyll content and degree of chlorosis of new leaves<sup>[73]</sup>. In the present study, transgenic lines had stronger FCR activity than WT, which may be attributed to the fact that *MhLHCB15* can promote Fe<sup>3+</sup> reduction and enhance iron utilization by increasing FCR activity. It was found that the Fe content of transgenic *A. thaliana* and apple calli was greater than that of WT under Fe deficiency stress, suggesting that *MhLHCB15* may modulate Fe uptake. This study also demonstrated that overexpressed apple calli pumped out more protons (H<sup>+</sup>) by acidification analysis. It showed that overexpressed apple calli may elevate the activity of the H<sup>+</sup>-ATPase and lower the pH, thereby raising the solubility of iron<sup>[74]</sup>. To further investigate the role of *MhLHCB15* in the signaling pathway of Fe deficiency stress, the expression levels of iron uptake-related genes (AHA2, AHA8, FRO2, IRT1, FIT, and FER) and chlorophyll synthases (HEMA1, GSA1, and CAO) in transgenic lines were assayed by qRT-PCR, and the expression of *MhLHCB15*-OE was higher than that of WT. All the above results indicated that *MhLHCB15* enhanced the tolerance of *A. thaliana* and apple calli to Fe deficiency stress.

### Yeast two-hybrid analysis of *MhLHCB15* gene

Protein interactions are one of the crucial mechanisms for their regulatory roles in organisms and proteins have a vital role in the reception of internal and external signals by cells and in the regulation of gene expression through signaling pathways<sup>[75]</sup>. In addition, most proteins need to work in concert with chaperone molecules or other protein complexes when exercising their functions. To deeply analyze the response mechanism of *MhLHCB15* under Fe deficiency stress, the present study utilized yeast two-hybrid technology to screen five proteins interacting with it. Using the NCBI database, the corresponding sequences of the five proteins were found and obtained, which were SGR1, THF1, NDUFS1, CSN5b, and LHCA3 proteins.

The stay-green gene SGR is a pivotal regulator of green organ senescence and maturation which are mainly involved in the regulation of chlorophyll degradation metabolism<sup>[76]</sup>. SGR1 can interact with LHCI protein and CCEs to form SGR1-CCE-LHCI macromolecular complex, which can be metabolized through chlorophyll catabolism pathway, thus significantly reducing the damage of aging to subcellular structure<sup>[35]</sup>. THF1 is widely distributed in multiple components of chloroplasts, and it was found that silencing the THF1 gene attenuated the degradation of LHCI proteins and

delayed the chlorosis of plant leaves<sup>[34]</sup>. NDUFS1 has a composition that includes NADH dehydrogenase and a series of iron-sulfur proteins (iron-sulfur centers)<sup>[77]</sup>. Deletion of NDUFS1 in plants causes severe inhibition of growth, but mutants can still survive<sup>[78]</sup>. CSN5b, a key component in the COP9 signaling complex, performs a crucial role in plants as well that is involved in the regulation of multiple signaling pathways<sup>[79]</sup>. In *A. thaliana*, CSN5b negatively regulates plant resistance to salt stress by interacting with VTC1 protein, which leads to the inhibition of ascorbic acid synthesis<sup>[80]</sup>. In summary, all these proteins were found to be associated with abiotic stress and photosynthesis.

In this study, the recombinant plasmid pGKB7-*MhLHCB15* was co-transfected into Y2HGold yeast receptor cells with pGAD7-SGR1, pGAD7-THF1, pGAD7-NDUFS1, pGAD7-CSN5b, and pGAD7-LHCA3, respectively, and the results showed that on SD/-Trp/-Leu medium growth and blue spot growth on SD/-Trp/-Leu/-Ade/-His/X- $\alpha$ -gal plates, therefore, it can be concluded that there may be an interplay between *MhLHCB15* and SGR1, THF1, NDUFS1, CSN5b, and LHCA3 proteins, demonstrating that these proteins may simultaneously regulate the photosynthesis of the plant to defend against iron deficiency stress.

### Conclusions

The 33 *MhLHC* family members were identified based on the apple genome database. The analysis of *cis*-element action demonstrated that the functions of the *MhLHC* protein may include a variety of biological processes such as the regulation of plant growth and development, phytohormone signaling, and plant resistance to stresses. The qRT-PCR results showed that *MhLHCB15* responded considerably to Fe deficiency stress. Meanwhile, the overexpression of the *MhLHCB15* gene has the biological functions of promoting chlorophyll synthesis, improving light-trapping capacity and enhancing photosynthetic performance; increasing iron uptake and utilization efficiency and antioxidant enzyme activities under iron deficiency stress, promoting iron reduction capacity and proton secretion capacity, and positively regulating iron deficiency resistance in transgenic *A. thaliana* and apple calli. The results of Y2H showed that *MhLHCB15* interacted with photosynthesis-related SGR1, THF1, NDUFS1, CSN5b, and LHCA3 proteins.

### Author contributions

The authors confirm contribution to the paper as follows: study conception and design: Dong Y, Wang Y; data collection: Dong Y, Zhang D, Zhao W; analysis and interpretation of results: Dong Y, Cheng J, Zhang Z; draft manuscript preparation: Dong Y, Wang X. All authors reviewed the results and approved the final version of the manuscript.

### Data availability

All data generated or analyzed during this study are included in this published article and its supplementary information files.

### Acknowledgments

This work were supported by the National Natural Science Foundation of China (Grant No. 32160696 and No.32460735).

### Conflict of interest

The authors declare that they have no conflict of interest.

**Supplementary information** accompanies this paper at (<https://www.maxapress.com/article/doi/10.48130/frures-0024-0039>)

## Dates

Received 14 June 2024; Revised 9 July 2024; Accepted 13 July 2024; Published online 20 February 2025

## References

1. Tabata R, Kamiya T, Imoto S, Tamura H, Ikuta K, et al. 2022. Systemic regulation of iron acquisition by *Arabidopsis* in environments with heterogeneous iron distributions. *Plant and Cell Physiology* 63:842–54
2. Zargar SM, Agrawal GK, Rakwal R, Fukao Y. 2015. Quantitative proteomics reveals role of sugar in decreasing photosynthetic activity due to Fe deficiency. *Frontiers in Plant Science* 6:592
3. Zhang X, Zhang D, Sun W, Wang T. 2019. The adaptive mechanism of plants to iron deficiency via iron uptake, transport, and homeostasis. *International Journal of Molecular Sciences* 20:2424
4. Briat JF, Dubos C, Gaymard F. 2015. Iron nutrition, biomass production, and plant product quality. *Trends in Plant Science* 20:33–40
5. Chen HM, Wang YM, Yang HL, Zeng QY, Liu YJ. 2019. NRAMP1 promotes iron uptake at the late stage of iron deficiency in poplars. *Tree Physiology* 7:1235–50
6. İncesu M, Yeşiloğlu T, Tuzcu O, Çimen B. 2015. Differential tolerance to iron deficiency of citrus rootstocks grown in calcareous soil. *Acta Horticulturae* 1065:1431–36
7. Zhang ZX, Zhang R, Wang SC, Zhang D, Zhao T, et al. 2022. Identification of *Malus halliana* R2R3-MYB gene family under iron deficiency stress and functional characteristics of *MhR2R3-MYB4* in *Arabidopsis thaliana*. *Plant Biology* 24:344–55
8. Kawanabe S, Zhu T. 1991. Degeneration and conservational trial of *Aneurolepidium chinense* grassland in Northern China. *Japanese Journal of Grassland Science* 37:91–99
9. Cheng L, Zhao T, Wu YX, Wang H, Zhang ZX, et al. 2020. Identification of AP2/ERF genes in apple (*Malus × domestica*) and demonstration that *MdERF017* enhances iron deficiency tolerance. *Plant Cell, Tissue and Organ Culture* 143:465–82
10. Dotaniya ML, Meena HM, Lata M, Kumar K. 2013. Role of phytosiderophores in iron uptake by plants. *Agricultural Science Digest* 33:73–76
11. Fernández V, Del Río V, Abadía J, Abadía A. 2006. Foliar iron fertilization of peach (*Prunus persica* (L.) Batsch): effects of iron compounds, surfactants and other adjuvants. *Plant and Soil* 289:239–52
12. Wang FP, Wang XF, Zhang J, Ma F, Hao YJ. 2018. *MdMYB58* modulates Fe homeostasis by directly binding to the *MdMATE43* promoter in plants. *Plant and Cell Physiology* 59:2476–89
13. Han D, Wang Y, Zhang Z, Pu Q, Ding H, et al. 2017. Isolation and functional analysis of *MxC53*: a gene encoding a citrate synthase in *Malus xiaojinensis*, with functions in tolerance to iron stress and abnormal flower in transgenic *Arabidopsis thaliana*. *Plant Growth Regulation* 82:479–89
14. Han D, Zhang Z, Ni B, Ding H, Liu W, et al. 2018. Isolation and functional analysis of *MxNAS3* involved in enhanced iron stress tolerance and abnormal flower in transgenic *Arabidopsis*. *Journal of Plant Interactions* 13:433–41
15. Han D, Xu T, Han J, Liu W, Wang Y, et al. 2022. Overexpression of *MxWRKY53* increased iron and high salinity stress tolerance in *Arabidopsis thaliana*. *In Vitro Cellular & Developmental Biology - Plant* 58:266–78
16. Terry N, Abadía J. 1986. Function of iron in chloroplasts. *Journal of Plant Nutrition* 9:609–46
17. Kale R, Hebert AE, Frankel LK, Sallans L, Bricker TM, et al. 2017. Amino acid oxidation of the D1 and D2 proteins by oxygen radicals during photoinhibition of photosystem II. *Proceedings of the National Academy of Sciences of the United States of America* 114:2988–93
18. Rochaix JD. 2014. Regulation and dynamics of the light-harvesting system. *Annual Review of Plant Biology* 65:287–309
19. Zhao S, Gao H, Luo J, Wang H, Dong Q, et al. 2020. Genome-wide analysis of the light harvesting chlorophyll *a/b*-binding gene family in apple (*Malus domestica*) and functional characterization of *MdLhcb4.3*, which confers tolerance to drought and osmotic stress. *Plant Physiology and Biochemistry* 154:517–29
20. Zhang Q, Ma C, Wang X, Ma Q, Fan S, et al. 2021. Genome-wide identification of the light-harvesting chlorophyll *a/b* binding (Lhc) family in *Gossypium hirsutum* reveals the influence of *GhLhcb2.3* on chlorophyll *a* synthesis. *Plant Biology* 23:831–42
21. Elias E, Liguori N, Saga Y, Schäfers J, Croce R. 2021. Harvesting far-red light with plant antenna complexes incorporating chlorophyll *d*. *Biomacromolecules* 22:3313–22
22. Najafpour MM, Allakhverdiev SI. 2015. Recent progress in the studies of structure and function of photosystems I and II. *Journal of Photochemistry and Photobiology B: Biology* 152:173–75
23. Albanese P, Manfredi M, Meneghesso A, Marengò E, Saracoe G, et al. 2016. Dynamic reorganization of photosystem II supercomplexes in response to variations in light intensities. *Biochimica et Biophysica Acta (BBA) - Bioenergetics* 1857:1651–60
24. Aghdasi M, Schluepman H. 2009. Cloning and expression analysis of two photosynthetic genes, *PSI-H* and *LHCBI*, under trehalose feeding conditions in *Arabidopsis* seedlings. *Iranian Journal of Biotechnology* 7:179–187,190
25. Su X, Ma J, Wei X, Cao P, Zhu D, et al. 2017. Structure and assembly mechanism of plant C<sub>2</sub>S<sub>2</sub>M<sub>2</sub>-type PSII-LHCII super complex. *Science* 357:815–20
26. Zhu W, Xu L, Yu X, Zhong Y. 2022. The immunophilin CYCLOPHILIN28 affects PSII-LHCII supercomplex assembly and accumulation in *Arabidopsis thaliana*. *Journal of Integrative Plant Biology* 64:915–29
27. Yan M, Yuan Z. 2020. Genome-wide analysis of the family of light-harvesting chlorophyll *a/b*-binding proteins in pomegranate (*Punica granatum* L.). *Acta Horticulturae* 1297:647–52
28. Xia Y, Ning Z, Bai G, Li R, Yan G, et al. 2012. Allelic variations of a light harvesting chlorophyll *a/b*-binding protein gene (*LHCB1*) associated with agronomic traits in barley. *PLoS One* 7:e37573
29. Xu YH, Liu R, Yan L, Liu ZQ, Jiang SC, et al. 2012. Light-harvesting chlorophyll *a/b*-binding proteins are required for stomatal response to abscisic acid in *Arabidopsis*. *Journal of Experimental Botany* 63:1095–106
30. Andersson J, Wentworth M, Walters RG, Howard CA, Ruban AV, et al. 2003. Absence of the Lhcb1 and Lhcb2 proteins of the light-harvesting complex of photosystem II: effects on photosynthesis, grana stacking and fitness. *The Plant Journal* 35:350–61
31. Jiang Q, Xu ZS, Wang F, Li MY, Ma J, et al. 2014. Effects of abiotic stresses on the expression of *Lhcb1* gene and photosynthesis of *Oenothera javanica* and *Apium graveolens*. *Biologia Plantarum* 58:256–64
32. Deng YS, Kong FY, Zhou B, Zhang S, Yue MM, et al. 2014. Heterology expression of the tomato *Lelhcb2* gene confers elevated tolerance to chilling stress in transgenic tobacco. *Plant Physiology and Biochemistry* 80:318–27
33. Fan P, Feng J, Jiang P, Chen X, Bao H, et al. 2011. Coordination of carbon fixation and nitrogen metabolism in *Salicornia europaea* under salinity: comparative proteomic analysis on chloroplast proteins. *Proteomics* 11:4346–67
34. Zhan J, Zhu X, Zhou W, Chen H, He C, et al. 2016. Thf1 interacts with PS I and stabilizes the PS I complex in *Synechococcus* sp. PCC7942. *Molecular Microbiology* 102:738–51
35. Park SY, Yu JW, Park JS, Li J, Yoo SC, et al. 2007. The senescence-induced staygreen protein regulates chlorophyll degradation. *The Plant Cell* 19:1649–64
36. Peng L, Shikanai T. 2011. Supercomplex formation with photosystem I is required for the stabilization of the chloroplast NADH dehydrogenase-like complex in *Arabidopsis*. *Plant Physiology* 155:1629–39
37. Ganeteg U, Klimmek F, Jansson S. 2004. Lhca5 – an LHC-type protein associated with photosystem I. *Plant Molecular Biology* 54:641–51
38. Guo A, Hu Y, Shi M, Wang H, Wu Y, et al. 2020. Effects of iron deficiency and exogenous sucrose on the intermediates of chlorophyll biosynthesis in *Malus halliana*. *PLoS One* 15:e0232694
39. Han ZH, Wang Q, Shen T. 1994. Comparison of some physiological and biochemical characteristics between iron-efficient and iron-inefficient species in the genus *Malus*. *Journal of Plant Nutrition* 17:1257–64
40. Livak KJ, Schmittgen TD. 2001. Analysis of relative gene expression data using real-time quantitative PCR and the 2<sup>-ΔΔCT</sup> method. *Methods* 25:402–08

41. Hu DG, Sun MH, Sun CH, Liu X, Zhang QY, et al. 2015. Conserved vacuolar H<sup>+</sup>-ATPase subunit B1 improves salt stress tolerance in apple calli and tomato plants. *Scientia Horticulturae* 197:107–16
42. Fitter DW, Martin DJ, Copley MJ, Scotland RW, Langdale JA. 2002. *GLK* gene pairs regulate chloroplast development in diverse plant. *The Plant Journal* 31:713–27
43. Bradford MM. 1976. A rapid and sensitive method for the quantitation of microgram quantities of protein utilizing the principle of protein-dye binding. *Analytical Biochemistry* 72:248–54
44. Wu M, Liu H, Gao Y, Shi Y, Pan F, et al. 2020. The moso bamboo drought-induced 19 protein PheDi19-8 functions oppositely to its interacting partner, PheCDPK22, to modulate drought stress tolerance. *Plant Science* 299:110605
45. Romero-Puertas MC, Rodríguez-Serrano M, Corpas FJ, Gómez M, Del Río LA, et al. 2004. Cadmium-induced subcellular accumulation of O<sub>2</sub><sup>•-</sup> and H<sub>2</sub>O<sub>2</sub> in pea leaves. *Plant, Cell & Environment* 27:1122–34
46. Schikora A, Schmidt W. 2001. Iron stress-induced changes in root epidermal cell fate are regulated independently from physiological responses to low iron availability. *Plant Physiology* 125:1679–87
47. Mandal Š, Banjanin B, Kujović I, Malenica M. 2015. Spectrophotometric determination of total iron content in black tea. *Bulletin of the Chemists and Technologists of Bosnia and Herzegovina* 44:29–32
48. Zhao Q, Ren YR, Wang QJ, Yao YX, You CX, et al. 2016. Overexpression of *MdbHLH104* gene enhances the tolerance to iron deficiency in apple. *Plant Biotechnol Journal* 14:1633–45
49. Hey D, Grimm B. 2018. ONE-HELIX PROTEIN2 (OHP2) is required for the stability of OHP1 and assembly factor HCF244 and is functionally linked to PSII biogenesis. *Plant Physiology* 177:1453–72
50. Alboresi A, Caffarri S, Nogue F, Bassi R, Morosinotto T. 2008. *In silico* and biochemical analysis of *Physcomitrella patens* photosynthetic antenna: identification of subunits which evolved upon land adaptation. *PLoS One* 3:e2033
51. Zhao Y, Kong H, Guo Y, Zou Z. 2020. Light-harvesting chlorophyll a/b-binding protein-coding genes in jatropha and the comparison with *Castor*, *Cassava* and *Arabidopsis*. *Peer J* 8:e8465
52. Umate P. 2010. Genome-wide analysis of the family of light harvesting chlorophyll a/b-binding proteins in *Arabidopsis* and rice. *Plant Signaling & Behavior* 5:1537–42
53. Singh J, Pandey P, James D, Chandrasekar K, Achary VMM, et al. 2014. Enhancing C3 photosynthesis: an outlook on feasible interventions for crop improvement. *Plant Biotechnology Journal* 12:1217–30
54. Kong F, Zhou Y, Sun P, Gao M, Li H, et al. 2016. Identification of light-harvesting chlorophyll a/b-binding protein genes of *Zostera marina* L. and their expression under different environmental conditions. *Journal of Ocean University of China* 15:152–62
55. Liu R, Xu YH, Jiang SC, Lu K, Lu YF, et al. 2013. Light-harvesting chlorophyll a/b-binding proteins, positively involved in abscisic acid signaling, require a transcription repressor, WRKY40, to balance their function. *Journal of Experimental Botany* 64:5443–56
56. Girardi CL, Rombaldi CV, Cero JD, Nobile PM, Laurens F, et al. 2013. Genome-wide analysis of the AP2/ERF superfamily in apple and transcriptional evidence of ERF involvement in scab pathogenesis. *Scientia Horticulturae* 151:112–21
57. Fujita Y, Yoshida T, Yamaguchi-Shinozaki K. 2013. Pivotal role of the AREB/ABF-SnRK2 pathway in ABRE-mediated transcription in response to osmotic stress in plants. *Physiologia Plantarum* 147:15–27
58. Luo J, Abid M, Tu J, Gao P, Wang Z, et al. 2022. Genome-wide identification of the *LHC* gene family in kiwifruit and regulatory role of *Aclhcb3.1/3.2* for chlorophyll a content. *International Journal of Molecular Sciences* 23:6528
59. Myouga F, Takahashi K, Tanaka R, Nagata N, Kiss AZ, et al. 2018. Stable accumulation of photosystem II requires ONE-HELIX PROTEIN1 (OHP1) of the light harvesting-like family. *Plant Physiology* 176:2277–91
60. Wu R, Ran K, Zhao S, Cheng F. 2023. Genome-wide identification of the light-harvesting chlorophyll a/b binding protein gene family in *Pyrus bretschneideri* and their transcriptomic features under drought stress. *Horticulturae* 9:522
61. Saito A, Shimizu M, Nakamura H, Maeno S, Katase R, et al. 2014. Fe deficiency induces phosphorylation and translocation of Lhcb1 in barley thylakoid membranes. *FEBS Letters* 588:2042–48
62. Zuo Z, Chen Z, Zhu Y, Bai Y, Wang Y. 2014. Effects of NaCl and Na<sub>2</sub>CO<sub>3</sub> stresses on photosynthetic ability of *Chlamydomonas reinhardtii*. *Biology* 69:1314–22
63. Farquhar GD, Sharkey TD. 1982. Stomatal conductance and photosynthesis. *Annual Review of Plant Physiology* 33:317–45
64. Mafakheri A, Siosemardeh A, Bahramnejad B, Struik PC, Sohrabi Y. 2010. Effect of drought stress on yield, proline and chlorophyll contents in three chickpea cultivars. *Australian Journal of Crop Science* 4:580–85
65. Ji S, Zhang Y, Xu M, Zhao M, Chen H, et al. 2024. Characterization of low-temperature sensitivity and chlorophyll fluorescence in yellow leaf mutants of tomato. *Agronomy* 14:2382
66. Maxwell K, Johnson GN. 2000. Chlorophyll Fluorescence—a practical guide. *Journal of Experimental Botany* 51:659–68
67. Ali S, Xu Y, Jia Q, Ma X, Ahmad I, et al. 2018. Interactive effects of plastic film mulching with supplemental irrigation on winter wheat photosynthesis, chlorophyll fluorescence and yield under simulated precipitation conditions. *Agricultural Water Management* 207:1–14
68. Miller G, Suzuki N, Ciftci-Yilmaz S, Mittler R. 2010. Reactive oxygen species homeostasis and signaling during drought and salinity stresses. *Plant, Cell & Environment* 33:453–67
69. Javaux M, Schroder T, Vanderborght J, Vereecken H. 2008. Use of a three-dimensional detailed modeling approach for predicting root water uptake. *Vadose Zone Journal* 7:1079–88
70. Rahdari P, Tavakoli S, Hosseini SM. 2012. Studying of salinity stress effect on germination, proline, sugar, protein, lipid and chlorophyll content in Purslane (*Portulaca oleracea* L.) leaves. *Journal of Stress Physiology & Biochemistry* 8:182–93
71. Zhang L, Wang X, Shi Q, Gao Q, Liu Z. 2008. Differences of physiological responses of cucumber seedlings to NaCl and NaHCO<sub>3</sub> stress. *Chinese Journal of Applied Ecology* 19:1854–59
72. Tang L, Cai H, Ji W, Luo X, Wang Z, et al. 2013. Overexpression of *GsZFP1* enhances salt and drought tolerance in transgenic alfalfa (*Medicago sativa* L.). *Plant Physiology and Biochemistry* 71:22–30
73. Incesu M, Yesiloglu T, Tuzcu O, Cimen B, Yilmaz B. 2016. Response of *Citrus* rootstocks to iron deficiency under high pH conditions. *Citrus Research & Technology* 37:66–75
74. Santi S, Schmidt W. 2009. Dissecting iron deficiency-induced proton extrusion in *Arabidopsis* roots. *New Phytologist* 183:1072–84
75. Waadt R, Schmidt LK, Lohse M, Hashimoto K, Kudla J. 2008. Multicolor bimolecular fluorescence complementation reveals simultaneous formation of alternative CBL/CIPK complexes *in planta*. *The Plant Journal* 56:505–16
76. Barry CS, McQuinn RP, Chung MY, Besuden A, Giovannoni JJ. 2008. Amino acid substitutions in homologs of the STAY-GREEN protein are responsible for the *green-flesh* and *chlorophyll retainer* mutations of tomato and pepper. *Plant Physiology* 147:179–87
77. Garmier M, Carroll AJ, Delannoy E, Vallet C, Day DA, et al. 2008. Complex I dysfunction redirects cellular and mitochondrial metabolism in *Arabidopsis*. *Plant Physiology* 148:1324–41
78. Meyer EH, Tomaz T, Carroll AJ, Estavillo G, Delannoy E, et al. 2009. Remodeled respiration in *ndufs4* with low phosphorylation efficiency suppresses *Arabidopsis* germination and growth and alters control of metabolism at night. *Plant Physiology* 151:603–19
79. Zhou C, Wee S, Rhee E, Naumann M, Dubiel W, et al. 2003. Fission yeast COP9/signalosome suppresses cullin activity through recruitment of the deubiquitylating enzyme Ubp12p. *Molecular Cell* 11:927–38
80. Wang J, Yu Y, Zhang Z, Quan R, Zhang H, et al. 2013. *Arabidopsis* CSN5B interacts with VTC1 and modulates ascorbic acid synthesis. *The Plant Cell* 25(2):625–36



Copyright: © 2025 by the author(s). Published by Maximum Academic Press, Fayetteville, GA. This article is an open access article distributed under Creative Commons Attribution License (CC BY 4.0), visit <https://creativecommons.org/licenses/by/4.0/>.